mesh) and slurried with filtered bottom water. Three sterile flasks each received 500 ml of sediment slurry. The three flasks were as follows: control, amended with 400 μM NH_4^+; +S, pulsed with 100 μM HS^- twice daily; or S + N, amended with 400 μM NH_4^+ and pulsed with 100 μM HS^- twice daily. During enrichment, hydrated air flowed continuously through the cultures. Approximately 24 hours after the last HS^- pulse was administered, nitrification rates were assessed in subsamples amended with either 150 or 400 μM NH_4^+.

12. M. B. Goldhaber and I. R. Kaplan, *Soil Sci.* **119**, 42 (1975); W. Davidson, *Aquatic Sci.* **53**, 309 (1991).
13. J. P. Chanton, C. S. Martens, M. B. Goldhaber, *Geochim. Cosmochim. Acta* **51**, 1187 (1987).
14. Surface sediments (0 to 3 cm) were sieved, homogenized, and randomly distributed [1 gws (gram of wet sediment)] into 40-ml serum bottles. Thirty milliliters of filtered seawater, amended with 300 μM NH_4^+, was added to each bottle; 18 replicates were prepared for each treatment group. Treatment groups were as follows: control, NH_4^+ only; pH, pH adjusted with NaOH to match that in HS^--amended samples; goethite (G), amended with 700 μM goethite; HS^-, amended with 60 μM HS^-; and HS^- + G, amended with 60 μM HS^-, then with 700 μM goethite. Triplicate samples from each group were collected and analyzed at approximately 0.5, 3, 6, 12, and 23 hours. Sulfide was determined as in (*24*). We quantified oxygen concentration by inserting microelectrodes (Diamond General, Ann Arbor, MI) into bottles before collecting nutrient samples. Oxygen was not limiting during these experiments. NO_x concentration was determined as described previously (*10*).
15. D. E. Canfield, *Geochim. Cosmochim. Acta* **53**, 619 (1989).
16. W. M. Kemp *et al.*, *Limnol. Oceanogr.* **35**, 1545 (1990).
17. J. I. Hansen, K. Henriksen, B. B. Jørgensen, *Microb. Ecol.* **7**, 297 (1981).
18. J. M. Caffrey, N. P. Sloth, H. F. Kaspar, T. H. Blackburn, *FEMS Microbiol. Ecol.* **12**, 159 (1993).
19. G. E. Hall, in *Nitrification*, J. I. Prosser, Ed. (IRL Press, Washington, DC, 1986), pp. 127–155.
20. P. Sampou and C. A. Oviatt, *Mar. Ecol. Prog. Ser.* **72**, 271 (1992).
21. J. Sørensen, L. K. Rasmussen, I. Koike, *Can. J. Microbiol.* **33**, 1001 (1987).
22. C. F. D'Elia, J. G. Sanders, W. R. Boynton, *Can. J. Fish. Aquatic Sci.* **43**, 397 (1986); T. C. Malone *et al.*, *Estuaries*, in press.
23. M. Jones, *Water Res.* **18**, 643 (1984).
24. J. D. Cline, *Limnol. Oceanogr.* **14**, 454 (1969).
25. This work was supported by the U.S. NSF's Land Margin Ecosystems Research (LMER) Program. We thank members of the Tomales Bay LMER group for field assistance and R. Chambers, J. Cornwell, W. Kimmerer, L. Miller, S. Smith, B. Ward, and two anonymous reviewers for critical comments. We also thank B. Ward for discussions and suggestions.

21 April 1995; accepted 5 September 1995

Cross-Arc Geochemical Variations in the Kurile Arc as a Function of Slab Depth

Jeffrey G. Ryan,* Julie Morris,† Fouad Tera, William P. Leeman, Andrei Tsvetkov

Lavas from transects across the Kurile Islands arc showed geochemical variations related to changes in the compositions of fluids derived from the subducting slab. Enrichment factors for boron, cesium, arsenic, and antimony, all elements with strong affinities for water, decreased across the arc. This decrease is presumably related to losses of water-rich fluids during the dehydration of the subducting plate. Enrichments of potassium, barium, beryllium-10, and the light rare earth elements remained constant; these species may move in silica-rich fluids liberated from the slab at greater depths.

The involvement of slab-derived melts (*1*, *2*) and the importance of nonmagmatic (that is, fluid) slab components (*3*–*6*) in arc magmatism are uncertain and much debated. Only recently have clear indicators for slab contributions been identified: High concentrations of B and ^{10}Be in arc lavas require material inputs to arc source regions from subducted oceanic sediments and altered oceanic crust (*4*, *7*). To better understand magma generation at arcs and the significance of subduction in crustal recycling, we need to know what processes control material fluxes from the subducting plate and how these fluxes interact with the overlying mantle.

We examined trace element systematics in suites of lavas from a series of "cross-arc transects" across the arc of the Kurile Islands. The volcanoes sampled lie 120 to 250 km above the subducting plate and may thus reflect slab-mantle interactions occurring over a range of pressure and temperature conditions. The Kurile Islands are a stereotypic island arc, erupting medium K calc-alkaline lavas across an unusually wide volcanic zone (Table 1) (*8*). Most Kurile lavas that have been analyzed have ^{10}Be contents greater than 1.0×10^6 atoms/g, which indicates subducted sediment (slab) involvement during magma genesis. Limited isotopic variation ($^{87/86}Sr \approx 0.703$ to 0.7034 and $^{143/144}Nd \approx 0.5130$ to 0.5131) (*9*) suggests that neither enriched mantle sources nor crustal assimilation strongly affects lava chemistry.

Data for six Kurile Islands cross-arc transects are presented in Table 1 and Fig. 1 (*10*). Incompatible trace elements show a spectrum of across-arc variation patterns. B and Sb (*11*) reflect one extreme (Fig. 1A)—high concentrations in volcanic front (VF) lavas, with abundances declining across the arc. Cs and Rb (Fig. 1C) show no clear pattern of concentration variation, whereas K, Ba, and most other elements (Fig. 1, E and G) increase in concentration across the arc. These element abundance patterns result from slab inputs, which may vary with increasing slab depth, and from varying extents of partial melting and crystal fractionation. We disentangled these effects by determining the ratios of the elements of interest to other elements with similar solid-melt distribution coefficients (*D*s) but much lower apparent solid "slab fluid" *D*s. Use of these element ratios minimized the effects of processes other than subduction modification of the mantle. K_2O, La, and B all have solid or melt *D*s similar to that of Be; the solid or melt *D* for Cs is more similar to that of Th. Thus, in

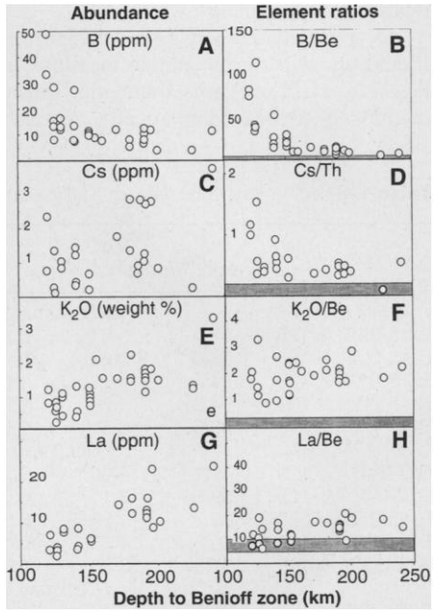

Fig. 1. Plots of element abundance and ratios for cross-arc transects in the Kurile Islands. Depths to Benioff zone were determined with the use of data from (*32*) and (*33*); absolute uncertainties in depths are ±10 km, but volcano-to-volcano uncertainties are much smaller. Gray fields on ratio diagrams represent ranges for mid-ocean ridge basalt and Ocean island basalt sources based on (*5*) and (*35*) and references therein. (**A** and **B**) B and B/Be versus depth. (**C** and **D**) Cs and Cs/Th versus depth. (**E** and **F**) K_2O and K_2O/Be versus depth. (**G** and **H**) La and La/Be versus depth.

J. G. Ryan, Department of Geology, University of South Florida, Tampa, FL 33620, USA, and Department of Terrestrial Magnetism, Carnegie Institution of Washington, Washington, DC 20015, USA.
J. Morris and F. Tera, Department of Terrestrial Magnetism, Carnegie Institution Washington, Washington, DC 20015, USA.
W. P. Leeman, Department of Geology and Geophysics, Rice University, Houston, TX, USA.
A. Tsvetkov, Institute of Mining and Mineral Resources, Russian Academy of Sciences, Moscow, Russia.

*To whom correspondence should be addressed.
†Present address: Department of Earth and Planetary Sciences, Washington University, St. Louis, MO, USA.

Fig. 1, B/Be, Cs/Th, K_2O/Be, and La/Be ratios are plotted versus depth.

It can be demonstrated that lavas erupting at the rear of an arc are produced by generally lower degrees of partial melting than are those at the VF (*12*). This effect will produce positive slopes on abundance diagrams, both when no slab-related elemental inputs are evident and when inputs are constant across the arc (Fig. 2A). In either case, ratio diagrams (Fig. 2B) show subhorizontal trends versus slab depth, with trend positions shifted to values higher than those of the normal upper mantle if inputs from the slab have occurred. K and Ba behave as if approximately constant subduction additions occur across the arc, whereas La shows only slight enrichments relative to upper mantle values.

As a highly incompatible element, B should show patterns similar to those in Figs. 2A or 2B, unless its abundance in the mantle decreases dramatically enough across the arc to mask the effects on B concentration of lower degrees of melting behind the front (Fig. 2, C and D). B/Be ratios decline from as high as 125 at the VF to <10 in the rearmost volcanoes, which suggests that inventories of slab-derived B in the mantle decrease across the arc (Fig. 1B). Cs/Th ratios (Fig. 1D) show less pronounced but significant across-arc declines, which indicates that mantle wedge Cs inventories show comparable changes. The patterns of B/Be and Cs/Th variation across the Kurile Islands resemble changes observed in subduction-related metamorphic massifs such as the Catalina Schist (*13*, *14*), where reductions in B and Cs concentrations as grade increases correlate with decreases in N and H_2O concentrations.

The Kurile Islands results demonstrate that slab signatures extend beyond VF source regions beneath arcs, and that transport of these signatures into behind-the-front (BTF) sources produces specific elemental fractionations. Mechanisms for slab-mantle chemical exchange beneath arcs must explain the differing trace element variation patterns observed across the Kuriles. Inputs of slab sediment melts will explain enrichments of K, Ba, Sr, and La in arc lavas (*2*), but cannot reconcile across-arc changes in the abundances of similarly incompatible elements such as B. Metamorphic devolatilization processes progressively remove B and Cs from the slab sediments beginning at relatively low grades (*13–17*), but do not substantially mobilize K or Ba over the same range of pressure and temperature. Fluids derived from metamorphosing oceanic crust have been proposed to balance the Sr and Pb budgets of arcs (*18*) and to explain B isotope systematics across arcs (*19*). Such fluids could both trigger sediment melting and enrich the melts in fluid-soluble species. However, B and Cs abundances in old ocean crust are much lower than in trench sediments (*2*, *20*). Also, the high ^{10}Be concentrations and $^{10}Be/^{9}Be$ ratios in Kurile Islands lavas require slab inputs in which 100% of the ^{10}Be is provided by subducted sediments (*4*). Thus, it is likely that large amounts of B and of most other trace elements added to arc source regions are derived from subducted sediments, the origins of slab fluids notwithstanding.

Current models of subduction zone chemical exchanges envision the slab input process as a point-source event, with the slab signature transported either downdip in hydrated mantle near the slab (*21*) or subhorizontally through the wedge to magmatic source regions (*22*). The horizontal trans-

Table 1. Selected elemental data for Kurile Islands transects. Dashes indicate no analysis.

Sample	Slab depth	SiO_2 (weight %)	MgO (weight %)	K_2O (weight %)	B (ppm)	Be (ppm)	Ba (ppm)	Cs (ppm)	La (ppm)	Th (ppm)	Sb (ppm)	As (ppm)
North Iturup transect (45° to 46°N)												
B-15-392	125	57.4	5.51	0.77	29.0	0.23	191	1.4	4.5	0.9	*0.44*	*4.7*
B-15-394	125	51.0	3.63	0.27	8.6	0.22	86	0.18	2.5	0.3	*0.11*	*1.2*
B-15-81/1	170	54.3	4.77	1.66	12.9	0.84	378	1.8	14.9	4.6	*0.10*	*0.78*
B-15-80/5	190	64.6	1.37	1.22	8.6	0.71	281	1.1	11.8	3.0	*0.07*	*0.48*
B-15-73/1	240	60.6	3.51	3.56	12.2	1.55	629	3.8	24.3	6.6	*0.10*	*0.88*
South Iturup transect (44° to 45°N)												
B17-643	125	49.1	4.80	0.15	5.1	0.19	275	0.56	1.1	0.2	–	–
B17-642	125	59.6	3.11	0.63	13.8	0.41	365	0.34	3.7	0.9	0.17	2.4
B-15-356	125	65.7	1.38	0.88	16.0	0.52	242	–	–	–	–	–
B17-640	140	50.2	4.25	0.46	8.7	0.45	319	0.41	4.1	0.4	–	–
B17-34/1	195	57.8	3.88	1.95	12.4	1.11	844	2.9	23.4	7.6	0.07	0.90
Chirpoy transect (46°30'N)												
B-15-325	140	60.7	3.10	1.42	28.0	0.53	237	1.5	9.2	2.6	*0.4*	*5.1*
B-17-684	140	51.1	5.05	0.60	8.2	0.33	138	0.47	4.9	1.0	*0.08*	*0.92*
B-17-603	225	52.3	7.70	1.40	4.5	0.75	341	0.31	14.0	2.7	*0.05*	*0.44*
Chirinkotan transect (48° to 49°N)												
B-11-112/9	130	55.3	4.27	1.06	12.6	0.52	246	1.1	7.9	2.4	0.07	1.7
B-11-111/7	130	56.8	3.67	0.48	16.9	0.42	137	–	–	–	–	–
B-11-111/3	130	59.4	3.52	1.14	12.9	1.26	276	0.80	8.4	2.1	0.17	0.95
B-11-569	150	56.3	4.13	1.05	10.3	0.43	239	–	–	–	–	–
B-11-570	150	58.5	4.00	1.25	14.7	0.51	432	1.2	6.2	1.7	0.09	2.0
B-11-527	190	56.3	2.80	1.95	13.0	0.89	638	2.7	8.4	4.9	–	0.89
Onekotan transect (49°15' to 50°N)												
H-3	120	61.5	2.08	0.88	34.1	0.46	269	0.82	3.8	0.8	*0.54*	*5.7*
8322/3	120	64.7	1.93	1.31	49.6	0.61	307	2.4	7.7	2.0	*0.70*	*9.2*
B11-81/4	155	60.1	3.19	2.29	9.4	0.93	725	2.3	14.1	5.1	–	1.3
B-11-504	160	56.6	4.74	1.67	8.4	0.77	436	–	–	–	–	–
B-11-75/4	180	52.2	4.47	1.58	8.9	0.73	399	1.4	12.7	3.0	*0.09*	*0.87*
B-11-73/13	180	62.4	2.41	2.43	–	0.96	657	2.9	16.3	6.5	0.11	2.0
B11-74/1	180	50.9	5.21	1.65	5.9	0.64	499	0.91	10.5	2.3	–	–
B-11-72/3	200	48.0	5.24	1.60	4.6	0.55	359	0.89	10.8	2.1	*0.04*	*0.57*
Paramushir-Alaid transect (50°30' to 51°N)												
4/2 81	150	58.4	3.40	1.17	10.7	0.68	420	–	–	–	–	–
B25-865	150	58.4	2.54	0.82	11.4	0.67	396	0.24	6.5	0.7	0.05	1.3
PARA 16-1	150	53.0	3.97	0.86	11.8	0.50	385	0.73	6.2	1.1	0.09	1.8
B-11-575	190	50.4	4.41	1.79	9.7	0.88	341	1.2	12.3	2.2	–	–
2/381	190	51.2	3.82	1.60	7.9	0.88	332	–	–	–	–	–
B-11-576	190	51.0	4.23	1.58	11.0	0.85	313	–	–	–	–	–
K-8	190	51.3	4.03	1.84	13.0	0.88	372	1.3	13.4	2.5	0.30	–
B-11-52/1	225	47.2	5.07	1.38	–	–	221	–	–	–	–	–
B-11-52/2	225	47.8	6.44	1.33	–	–	235	–	–	–	–	–

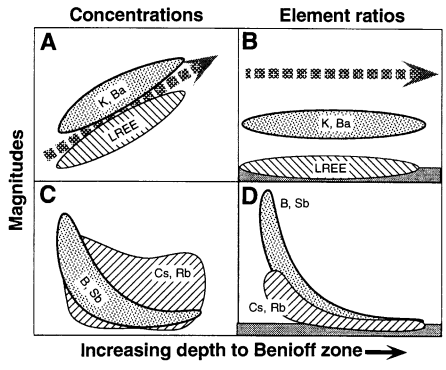

Fig. 2. Schematic illustration of concentration and ratio systematics. Fields depict lava concentration trends; arrows show trajectories produced by progressive variations in extents of melting or crystallization. LREE are the light rare earth elements. (**A** and **B**) Concentration and ratio patterns versus depth for trace elements, which show uniform or minimal inputs from the subducting plate over a range of depths. (**C** and **D**) Content and ratio patterns for elements such as B, in which inputs from the subducting plate vary as a function of slab depth. Gray regions in (B) and (D) represent ratio values for oceanic mantle sources.

port scenario requires that phases hosting slab-derived species survive melting events at the VF (and one or more BTF melting events) and that the observed elemental fractionations be generated largely through mineral-melt equilibria. However, many phases proposed to host slab fluids in the wedge [for example, antigorite, lawsonite, and "phase A" (*23*, *24*)] decompose well below sub-arc melting temperatures. Amphibole and phlogopite are stable at higher temperatures but will be preferentially consumed during melting. Transport of fluids in the absence of hydrous phases (that is, as H_2O dissolved in "dry" mantle minerals) also seems unlikely, as the solid-melt distribution behavior of H_2O is similar to that of Ce (*25*). Arc melting would thus extract H_2O, K, B, and other incompatibles from the mantle with similar efficiency, precluding substantial across-arc fractionations.

Transport of the slab signature in hydrated mantle near the slab circumvents thermal stability problems, but requires that partitioning between solids and fluids during mineral decompositions generate across-arc elemental fractionations. Experimental results on antigorite decomposition suggest an inverse correlation between the ionic radius and the solid-fluid partition coefficient for alkaline elements (*23*). However, new data for subduction-related serpentines suggest that antigorite may be a poor host for Ba and K (*26*). Lawsonite hosts Sr well but hosts other alkaline elements only poorly; amphiboles and phlogopites, however, may retain inventories of K, Ba, and other alkaline species (*24*, *27*). B partitions strongly into serpentines (*26*) and may partition modestly into lawsonite (*24*), but B partitioning affinities into amphibole or phlogopite (and the partitioning of Sb or As into any of the above phases) are unknown. To generate the across-arc changes in B and like species, however, the solid-fluid partition coefficients of these elements during mantle dehydration must be <1, so that slab-derived inventories are depleted with depth. An added constraint on all mantle transport models relates to observed ^{10}Be variations (*28*): Transport times from the VF to the rearmost centers in the Kurile Islands cannot exceed one ^{10}Be half-life. The slab signature must therefore travel into BTF source regions at a velocity comparable to that of the slab.

Implicit in the above models is the presumption that the slab dehydrates at depths too shallow to generate arc lavas. If, however, the slab can retain fluids to greater depths, complications such as the ^{10}Be timing constraint disappear. As mentioned above, B, Cs, N, and H_2O all show regular abundance declines with increasing pressures and temperatures in metamorphic massifs believed to represent emplaced portions of slabs. All of these species, and most other alkaline elements, are predominantly hosted by phengitic white micas (*24*). White mica persists over a large range of pressure and temperature conditions during metamorphism and may be stable to <200 km on the slab (*29*). Fluid compositions during slab dehydration would thus be controlled by white mica re-equilibrations with increasing depth, resulting in the liberation of B, Sb, and Cs (but not of K, Ba, or La) in hydrous fluids.

For an on-slab transport model to produce the across-arc elemental patterns of the Kurile Islands, a mechanism must also exist to mobilize elements such as K and La [and Be (*4*, *12*)], which appear not to partition strongly into fluids that transport B and Cs. Melts of slab sediments in response to mica dehydration are capable of mobilizing these species in appropriate relative proportions (*2*, *30*). It is thus possible that a mixed slab flux, composed of both hydrous fluids and sediment melts, is input to the mantle beneath the Kurile Islands and other arcs. High-grade rocks of the Catalina schist include both veins and pegmatites, which suggests that liberating two compositionally different "fluids" from the slab under the same pressure and temperature conditions is possible (*31*). Variations in element ratios among VF lavas may thus relate to differing proportions of fluid and melt inputs to VF sources, whereas BTF magmas may record the "drying out" of the slab as hydrous fluids (with B, Sb, and Cs) are driven off with increasing depth. Because all Kurile Islands lavas show similar K/Be and Ba/Be ratios, all source regions across the arc must receive inputs of compositionally similar melts. Minimum VF slab temperatures may thus be approximately equivalent to those encountered during amphibolite grade metamorphism. Sufficient B can persist on the slab at these temperatures to generate the elevated B/Be ratios observed in VF lavas from the Kurile Islands and other arcs (*13*, *17*). Further metamorphism with deeper subduction will drive off the remaining inventories of B and like elements, producing their depleting across-arc variation patterns. But melt inputs, even if reduced in magnitude in response to dehydration at depth, should maintain trace element signatures reflecting equilibration with slab residues.

REFERENCES AND NOTES

1. T. H. Green and A. E. Ringwood, *Contrib. Mineral. Petrol.* **18**, 105 (1968); B. D. Marsh and I. S. E. Carmichael, *J. Geophys. Res.* **79**, 1196 (1974); M. D. Defant and M. S. Drummond, *Nature* **347**, 662 (1990).
2. T. Plank and C. H. Langmuir, *Nature* **362**, 739 (1993).
3. R. L. Hickey-Vargas *et al.*, *J. Geophys. Res.* **91**, 5963 (1986).
4. J. D. Morris *et al.*, *Nature* **344**, 31 (1990).
5. J. G. Ryan and C. H. Langmuir, *Geochim. Cosmochim. Acta* **57**, 1489 (1993).
6. E. Stolper and S. Newman, *Earth Planet. Sci. Lett.* **121**, 293 (1994).
7. F. Tera *et al.*, *Geochim. Cosmochim. Acta* **50**, 535 (1986); J. D. Morris and F. Tera, *ibid.* **53**, 3197 (1989).
8. The subducting plate age is ≈120 million years; the slab dip is ≈ 45° (*32*); the subduction rate is 9 cm/year (*33*); and the crustal thickness is 15 to 25 km (*34*). Submarine Kurile volcanoes were dredged by the research vessel *Vulcanolog*.
9. J. C. Bailey *et al.*, *Contrib. Mineral. Petrol.* **95**, 155 (1987); D. Z. Zhuravlev *et al.*, *Chem. Geol.* **66**, 227 (1987).
10. Major element and trace element analyses were done by inductively coupled–plasma spectrometry (ICP) at the Department of Terrestrial Magnetism (DTM); some B data were collected by prompt gamma neutron activation analysis (PGNA) at McMaster University (Hamilton, Ontario, Canada). Analytical procedures were published in (*5*), (*15*), and (35). Analytical precision for ICP trace elements was B, ±10%; Be, Ba, and K, ±5%. Agreement between ICP and PGNA B data ≈ ± 10 to 15% at ≥5 ppm of B. Cs, Sb, As, Th, and rare earth elements were measured by instrumental neutron activation analysis at Oregon State University and Washington University; interlab comparisons suggest precision and agreement to ≈ ± 10 to 15%. Selected Sb and As data from the North Iturup, Chirpoy, and Onekotan transects (italicized in Table 1) were determined by P. Noll at the University of New Mexico and appeared previously in (*11*).
11. P. D. Noll *et al.*, *Geochim. Cosmochim. Acta*, in press.
12. A. G. Hochstaedter *et al.*, *Earth Planet. Sci. Lett.* **100**, 179 (1990).
13. G. Bebout, J. Ryan, W. Leeman, *Geochim. Cosmochim. Acta* **57**, 2227 (1993).
14. G. Bebout *et al.*, in preparation.
15. W. P. Leeman *et al.*, *Geochim. Cosmochim. Acta* **56**, 775 (1992).
16. S. R. Hart and M. R. Reid, *ibid.* **55**, 2379 (1991).
17. A.E. Moran, V. Sisson, W. Leeman, *Earth Planet. Sci. Lett.* **111**, 331 (1992).
18. R. M. Ellam and C. J. Hawkesworth, *Contrib. Mineral. Petrol.* **98**, 72 (1988); D. L. Miller, S. J. Goldstein, C. H. Langmuir, *Nature* **368**, 514 (1994).
19. T. Ishikawa and E. Nakamura, *Nature* **370**, 205 (1994); T. Ishikawa and F. Tera, *Eos* **75** (fall suppl.), 730 (1994).
20. T. W. Donnelly, G. Thompson, M. H. Salisbury, *Init. Rep. Deep Sea Drill Proj.* **51-53,** 1319 (1980).
21. Y. Tatsumi, *J. Geophys. Res.* **94**, 4697 (1989).
22. J. H. Davies and D. J. Stevenson, *ibid.* **97**, 2037 (1992); J. H. Davies and M. J. Bickle, *Philos. Trans. R. Soc. London A* **335**, 355 (1991).
23. Y. Tatsumi *et al.*, *J. Volc. Geotherm. Res.* **29**, 293 (1985).
24. K. J. Domanik *et al.*, *Geochim. Cosmochim. Acta* **57**, 4997 (1993).
25. P. J. Michael, *ibid.* **52**, 555 (1988).
26. P. Mattie and J. G. Ryan, *Eos* **75** (spring suppl.), 352 (1994).
27. J. Rosenbaum *et al.*, *Eos* **74** (fall suppl.), 680 (1993).
28. F. Tera *et al.*, *ibid.*, p. 674.
29. K. J. Domanik and J. R. Holloway, *ibid.*, p. 679.
30. M. C. Johnson and T. Plank, *ibid.*, p. 680.
31. G. E. Bebout, *Science* **251**, 413 (1991); ——— and M. D. Barton, *Geology* **17**, 976 (1989).
32. B. L. Isacks and M. Barazangi, in *Island Arcs, Deep Sea Trenches and Back-Arc Basins* (American Geophysical Union, Washington, DC, 1977), pp. 99–114.
33. J. B. Gill, *Orogenic Andesites and Plate Tectonics* (Springer-Verlag, New York, 1981).
34. T. Plank and C. H. Langmuir, *Earth Planet. Sci. Lett.* **90**, 349 (1990).
35. J. G. Ryan and C. H. Langmuir, *Geochim. Cosmochim. Acta* **52**, 237 (1988).

36. We thank O. Volnyets for help in obtaining samples, S. Shirey for aid and direction in the operation of the DTM ICP, and L. Haskin for INAA analyses. Supported by NSF grant EAR 90-04389 to J.M. and F.T., EAR 90-18996 to W.P.L., and EAR 92-19434 to S. Sacks and J.M.

1 May 1995; accepted 24 August 1995